https://doi.org/10.17221/57/2024-JFS

Assessment of ozone impact on forest vegetation using visible foliar injury, AOT40F exposure index and MDA concentration in two meteorologically contrasting years

Radek Novotný[1], Leona Vlasáková[2], Vít Šrámek[1], Václav Buriánek[1], Nina Benešová[2]*

[1]Forestry and Game Management Research Institute, Prague, Czech Republic
[2]Air Quality Division, Czech Hydrometeorological Institute, Prague, Czech Republic

**Corresponding author: novotny@vulhm.cz*

Citation: Novotný R., Vlasáková L., Šrámek V., Buriánek V., Benešová N. (2025): Assessment of ozone impact on forest vegetation using visible foliar injury, AOT40F exposure index and MDA concentration in two meteorologically contrasting years. J. For. Sci., 71: 40–56.

Abstract: This study aimed to evaluate ozone (O_3) phytotoxic potential using AOT40F (accumulated O_3 concentration over a threshold of 40 ppb for forest protection), document visible foliar O_3 injury across eight forest monitoring plots, analyse MDA (malondialdehyde) content in leaves and needles, and assess the relationship between visible injury and plot conditions. Initial findings are based on data from the 2021 and 2022 vegetation seasons. AOT40F values exceeded the critical level of 5 ppm·h^{-1} at all plots, with higher values in 2022. The correlation between AOT40F and visible injury was inconsistent; in 2021, minimal visible O_3 injuries were observed, while these were more frequent in 2022, notably on *Fagus sylvatica* leaves. The altitude effect on O_3 concentration indicates greater vegetation damage at higher altitudes. In contrast, the AOT40F-altitude relation was not significant. The 2021 vegetation season was characterised by lower temperatures and higher relative air humidity and soil moisture in comparison to 2022. Stomatal conductance conditions were similar in both years, except for lower soil moisture in 2022. Soil moisture, air humidity, and temperature together accounted for about 50% of the variance in visible injury in 2022. The findings suggest that the AOT40F capability for predicting damage to vegetation is limited and highlight the importance of future research focusing on stomatal O_3 flux-based approaches.

Keywords: European beech; malondialdehyde; Norway spruce; ozone

Ground-level ozone (referred to as O_3 throughout this paper) is a secondary photochemical pollutant. It is formed in complex photochemical chain reactions from its precursors, such as nitrogen oxides (NO_X), volatile organic compounds, carbon monoxide (CO) and methane (CH_4). These precursors come from both natural and anthropogenic sources (Nolle et al. 2002; The Royal Society 2008; Anav et al. 2016). O_3 formation is highly dependent on the meteorological situation; therefore, O_3 levels vary considerably from year to year (Cox, Chu 1993; Jacob et al. 1993). As a photochemical pollutant, ground-level O_3 depends on solar radiation intensity. Photochemical reactions of precur-

Supported by the ARAMIS project – Integrated System of Research, Evaluation and Control of Air Quality, and co-funded with the state support of the Technology Agency of the Czech Republic under the Environment for Life program (grant No. SS02030031). Within the article, ICP Forests data was used and evaluated with the institutional support of the Ministry of Agriculture (No. MZE-RO0123).

https://doi.org/10.17221/57/2024-JFS

sors under high temperatures lead to O_3 formation (Jacob, Winner 2009; Coates et al. 2016). O_3 is currently considered to be the most damaging common air pollutant to vegetation, with adverse effects on crop yield and forest health (Ashmore 2005; Cieslik 2009; Fares et al. 2017; EEA 2020).

Ozone may induce damage at the cell, leaf, organism or ecosystem level (Fuhrer 2002; Ashmore 2005; Ainsworth 2016; Emberson et al. 2018; Mills et al. 2018). Elevated O_3 concentrations also pose a threat to terrestrial biodiversity and ecosystem services (Mills et al. 2018; Agathokleous et al. 2020; Reif et al. 2023).

Ozone molecule enters the leaves through stomata and reacts rapidly in intercellular spaces (Fares et al. 2017). There, O_3 diffuses in the apoplast and rapidly decomposes to the reactive oxygen species (Pell et al. 1997; Schraudner et al. 1997; Mittler 2002). If the antioxidative system is not sufficient, biochemical and physiological changes in plants occur, and the plant is damaged (Ashmore 2003; Heath 2008; Fares et al. 2013; Emberson et al. 2018). Ozone exposure can result in visible foliar injury, accelerating leaf senescence, declining chlorophyll content, reduced photosynthetic activity, reduced carbon assimilation and biomass, increased crown defoliation, and increased sensitivity to other abiotic and biotic stresses (Pell et al. 1997; Ashmore 2003; Schaub et al. 2005; Wittig et al. 2009; Fares et al. 2013; Hoshika et al. 2013; Sicard et al. 2016; De Marco et al. 2017; Mills et al. 2018; Paoletti et al. 2019).

Foliar O_3 injury is a visible manifestation of internal physiological processes in leaves (Innes et al. 2001). Visible foliar injury is the first clear and unequivocal sign of the presence of phytotoxic levels of O_3 (Bergmann et al. 1999) and is not caused by any other co-occurring factors (Sicard et al. 2016). Visible foliar injury is the only evidence that can be detected visually by an expert in the field without the assistance of instrumentation (Paoletti et al. 2019). It is a reliable method for monitoring the effects of O_3 and estimating the potential risk to ecosystems under real field conditions (Bergmann et al. 1999; Schaub, Calatayud 2013). Visible foliar injury correlates better with phytotoxic ozone dose (POD; for more details regarding POD, see CLRTAP 2017), which is currently the best biologically meaningful O_3 metric, as compared to crown defoliation or radial growth (Paoletti et al. 2019).

Visible foliar O_3 symptoms appear on the upper, sun-exposed side of leaves, usually as the light-green or brown stippling and bronzing that later develops into larger brown areas. Severely affected leaves may curl, dry, and prematurely fall off. Later in the vegetation period, if the O_3 concentration is high, injury can also appear on the undersides of leaves. The intensity of reddening then increases, and the leaves may become entirely red. Symptoms appear always apart from the veins. The symptoms appear first on older and medium-aged leaves (i.e. an age effect). The overlapping leaves have a shadow effect, where the covered parts of the leaves remain green with no signs of damage (Innes et al. 2001).

Malondialdehyde (MDA), as a product of peroxidation of the cell-membrane lipids, is considered a biomarker of oxidative stress (Heath, Packer 1968; Uhlířová 1991; Davey et al. 2005). In several studies, MDA was used as an indicator of the O_3 impact on forest vegetation (Šrámek et al. 2007, Hůnová et al. 2010).

The air quality standard used for vegetation protection in Europe is the accumulated O_3 concentration over a threshold of 40 ppb (AOT40; EP 2008). AOT40 is calculated on an hourly basis for the vegetation period (forests 1 April – 30 September; crops and vegetation 1 April – 31 July) in daylight hours (i.e. between 8.00 and 20.00 Central European Time). This is because the exposure is generally limited to the period when stomata are open (Anav et al. 2016). The critical level (CL) of AOT40 for forests (AOT40F) is set at 5 ppm·h^{-1}. The CL of this index is usually exceeded in most parts of the Czech Republic (CHMI 2023b).

In the Czech Republic, O_3 has been monitored since 1993. Inter-annual variability in O_3 concentrations is high, depending strongly on meteorological conditions, in particular on global solar radiation, ambient air temperature and relative humidity, as demonstrated by long-term measurements in the Czech mountain forests (Hůnová et al. 2019a). The peak concentrations have decreased substantially due to reductions in precursor emissions (Hůnová, Bäumelt 2018). However, the O_3 levels are still high enough to affect ecosystems, including forests (Hůnová, Schreiberová 2012).

The objective of this study is to assess the phytotoxic potential of O_3 using the AOT40 exposure index, compare it to visible foliar symptoms in real forest stands, analyse MDA content in leaves and needles, and analyse the relationships between visible foliar injury, meteorological, and environmental conditions.

https://doi.org/10.17221/57/2024-JFS

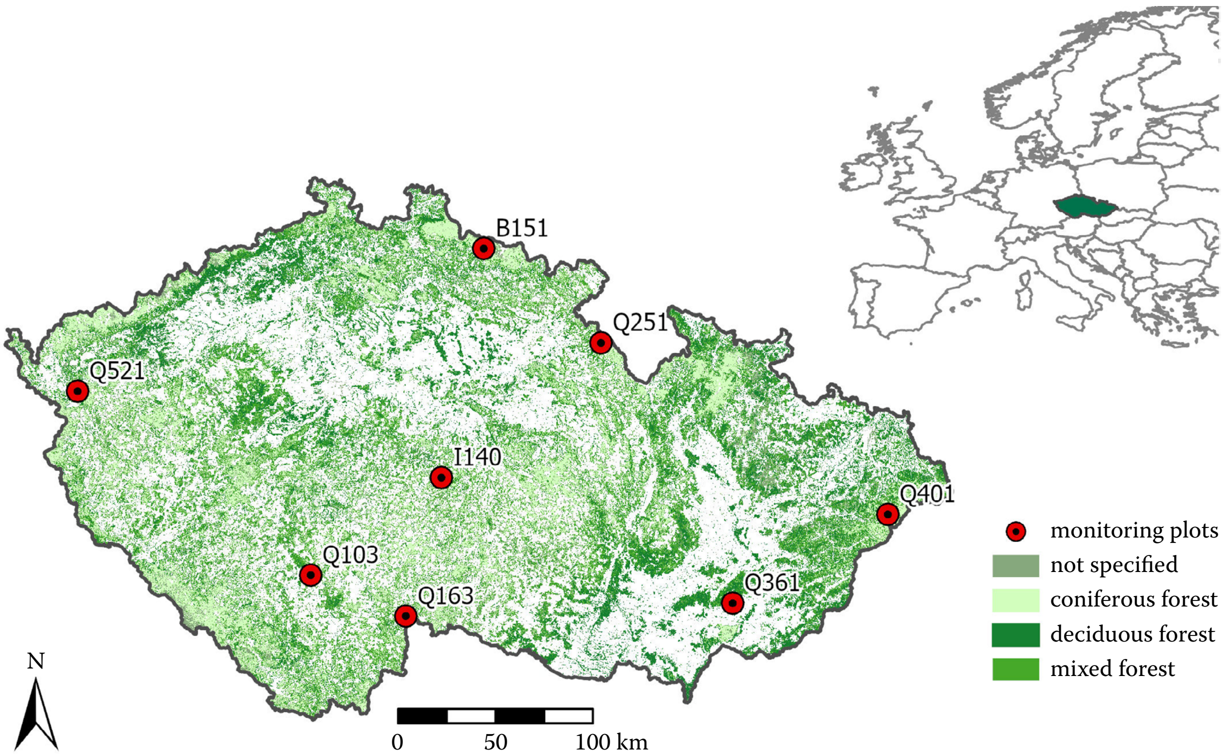

Figure 1. Plots with the visible foliar O_3 injury assessment

MATERIAL AND METHODS

Monitoring plots. Eight plots of intensive forest monitoring established within the ICP Forests (International Cooperative Programme on Assessment and Monitoring of Air Pollution Effects on Forests) programme have been selected in different regions of the Czech Republic at altitudes ranging from 350 m a.s.l. to 1 300 m a.s.l. (Figure 1; Table 1). These plots are suitable for our study because of the possibility of assessing visible foliar O_3 injury on a light-exposed forest edge at a distance of no more than 500 m from the monitoring plot. They are also fully equipped for meteorological data collection, six sites are also equipped for soil moisture measurement, and there is also a historical connection with older ground-level O_3 studies (Novotný et al. 2010; Boháčová et al. 2011; Šrámek et al. 2012). Attention

Table 1. Basic characteristics of evaluated plots

Plot code	Plot name	Main tree species	Position		Altitude (m a.s.l.)	Length of LESS (m)	Number of assessed 2 m × 1 m quadrates
B151	Mísečky	*Fagus sylvatica*	50.73°N	15.55°E	940	140	33
I140	Želivka	*Picea abies*	49.67°N	15.23°E	440	40	17
Q103	Všeteč	*Fagus sylvatica*	49.22°N	14.31°E	615	120	33
Q163	Lásenice	*Picea abies, Fagus sylvatica*	49.03°N	14.98°E	595	165	33
Q251	Luisino údolí	*Picea abies*	50.29°N	16.39°E	940	145	33
Q361	Medlovice	*Fagus sylvatica, Quercus petraea*	49.07°N	17.28°E	350	90	31
Q401	Klepačka	*Picea abies*	49.45°N	18.39°E	650	50	20
Q521	Lazy	*Picea abies*	50.05°N	12.63°E	875	90	31

LESS – light-exposed sampling site

https://doi.org/10.17221/57/2024-JFS

was paid to the main tree species with a special focus on Norway spruce [*Picea abies* (L.) Karst] and European beech (*Fagus sylvatica* L.). Other woody species, as well as shrubs and herbs, were also evaluated in terms of foliar injury.

Meteorological and soil moisture measurement. Basic meteorological parameters were measured continuously in an open area near the ICP Forests plot. The parameters were air temperature and air humidity (EMS 33H sensor), global solar radiation (EMS 11 pyranometer) (both produced by Environmental Measuring Systems s.r.o., Czech Republic), precipitation (Met One 370D rain gauge), and wind speed and wind direction (Met One 034B sensor) (both produced by Met One Instruments, USA). The placement of instruments and methods was in accordance with the ICP Forests manual (Raspe et al. 2020). Variables were measured in 1-minute intervals, and 10-minute averages were stored for further evaluation. Soil temperature (Pt100 thermometer; Environmental measuring systems s.r.o., Czech Republic), soil water content (Campbell CS616 soil moisture probe; Campbell Scientific, United Kingdom), and soil water potential (Delmhorst GB1 gypsum block; Delmhorst Instrument Co., USA) were measured within the monitoring plot at three soil depths: 10 cm, 30 cm, and 50 cm. Soil moisture content was measured in three repetitions, and water potential was measured in two repetitions. Data were recorded and stored in 30-minute intervals.

The parameters f_{temp}, f_{VPD}, f_{SW}, and f_{light} incorporate the effects of meteorological and environmental conditions on stomatal opening, i.e. the effect of temperature (f_{temp}), vapour pressure deficit (f_{VPD}), soil water (f_{SW}) and irradiance (f_{light}). That is, they are expressed as relative proportion functions to the maximum stomatal conductance in relative terms (i.e. they accept values between 0 and 1; CLRTAP 2017). These parameters take into account physiological minima, maxima, and optima of temperature (*Temp*), atmospheric water vapour pressure deficit, soil water, and global radiation (*GLRD*). Therefore, they allow for the modifying influence on stomatal conductance and provide a better characterisation of conditions for O_3 uptake (which subsequently may lead to vegetation damage) compared to measured meteorological and soil parameters. These parameters were calculated for *Fagus sylvatica* (because it is the main woody species along with *Picea abies* and the most frequently symptomatic species at our plots) according to the methodologies outlined in CLRTAP 2017.

O_3 concentrations and AOT40F (AOT40 for forest protection). The AOT40F values were calculated from hourly O_3 concentrations at a particulate plot for the vegetation season. Considering the usual leaf unfolding and autumn leaf colouring time of *Fagus sylvatica*, the evaluating period was set from 15 May to 30 September of the respective year. AOT40F (expressed in ppm·h^{-1}) was calculated as the sum of the difference between hourly concentrations greater than 40 ppb and 40 ppb over a given period using only the one-hour values of O_3 concentration between 8.00 and 20.00 Central European Time each day. Hourly concentrations in a 1 km × 1 km grid were calculated by combining O_3 concentration monitoring at rural stations, chemical transport model CAMx, and other supplemental data (altitude and five-year grided O_3 averages). The methodology for this combination was a linear regression model and subsequent kriging of the residuals obtained from this model (for more details, see Horálek et al. 2023).

Visible foliar O_3 injury assessment. The method of symptom assessment is described in detail in Schaub et al. (2020). The assessment was performed on light-exposed sampling site (LESS) plots. The LESS plots were exposed to full sunshine on an open plot area (i.e. forest edges), preferably on a south or southwest exposition. Each LESS plot was divided into not-overlapping quadrates (2 m × 1 m), and a given number of quadrates was randomly selected (depending on the length of the LESS plot). Visible foliar O_3 injury was assessed on fully developed leaves that were exposed to full sunlight.

The evaluation of leaf visual injury was carried out twice: in the late spring (June) and late summer (August–September) before natural leaf discolouration sets in. These evaluations covered both spring and summer O_3 peak concentrations with potentially adverse effects on vegetation (Monks 2000; Vingarzan 2004).

Assessment of O_3 foliar symptoms was conducted by two well-trained observers who regularly participate in the Field Ozone Intercalibration Course organised by ICP Forests. Several comparative documents were used to verify the O_3 effect (Innes et al. 2001; Novotný et al. 2009; Carrari et al. 2020) in order to exclude ambiguous symptoms caused by, such as fungal disease or heat stress (Novotný et al. 2009, Shaub et al. 2020).

MDA. For MDA determination, we used the method published by Heath and Packer (1968) with slight modifications. Regarding the high stability

https://doi.org/10.17221/57/2024-JFS

of MDA in both needles and leaves, and the large number of samples, we used air-dried needles/leaves (Uhlířová, Pasuthová 1993). Each sample consisted of 100–150 g of dried needles and leaves. Aqueous extracts from pulverised samples were prepared and heated in a water bath with thiobarbituric acid and trichloracetic acid solution at the final concentration of 0.3% and 12.5% (*w*/*v*). After the centrifugation, the MDA contents in the supernatant were analysed from the difference between the absorbance at the wavelength of 532 nm and 600 nm. The results are given as $\mu mol \cdot g^{-1}$ of dry matter. Two mixed samples for MDA analysis were prepared for each plot for Norway spruce: one mixed sample represented the current-year needles (further referred to as MDA-NS-cy), while the second represented the one-year-old needles (further referred to as MDA-NS-1y). *Fagus sylvatica* leaves were analysed as mixed samples (further referred to as MDA EB).

Statistics. The statistical analysis of the data was conducted using R (R Core Team 2020) and Statistica software (Version 12, 2013). The normality of the data was assessed using the Shapiro test. Differences in meteorological and environmental parameters, AOT40F, O_3 and MDA concentration levels between the 2021 and 2022 vegetation seasons were evaluated using the non-parametric Wilcoxon paired test. Differences in MDA content between *Fagus sylvatica* and *Picea abies* were tested using the Mann-Whitney *U*-test. The dependence of O_3 concentrations and AOT40F on altitude, the dependence of visible O_3 injury expressed as a percentage of symptomatic quadrates along LESS plots, and the percentage of symptomatic species at the plot on AOT40F were investigated using the non-parametric Spearman rank correlation test. The significance level chosen for the analysis was $P < 0.05$, indicating that results with *P*-values below this threshold were considered statistically significant. Multiple-factor analysis was used to detect the structure of the relationships between variables.

RESULTS

Meteorological and environmental conditions in 2021 and 2022. Meteorological and environmental conditions in 2021 and 2022 on our plots were characterised by air temperature (*Temp*), precipitation, *GLRD*, relative air humidity (*RAH*), and soil moisture (Table 2). In general, a significantly higher air temperature was found for the 2022 vegetation season. When examining individual plots, only plot Q521 demonstrated a statistically significantly higher temperature in 2022 compared to 2021. Correspondingly, a statistically higher value of *GLRD* was

Table 2. Characteristics of the 2021 and 2022 vegetation seasons: Average air temperature and average of daily maximal air temperature (*Temp*, *Max. temp*), total rainfall, average soil moisture at a depth of 10 cm, average relative air humidity (*RAH*), total global radiation (*GLRD*), AOT40F (accumulated O_3 concentration over a threshold of 40 ppb for forest protection), and seasonal average of O_3 concentrations for individual plots and collectively for all plots

Plot	*Temp* (°C)			*Max. temp* (°C)			Total precipitation (mm)			Soil moisture (%)			*RAH* (%)			*GLRD* ($kW \cdot m^{-2}$)			AOT40F ($ppm \cdot h^{-1}$)			O_3 (seasonal average, ppb)		
	2021	2022	*P*	2021	2022	*P*	2021	2022	*P*	2021	2022	*P*	2021	2022	*P*	2021	2022	*P*	2021	2022	*P*	2021	2022	*P*
B151	12.9	13.5	–	17.6	18.7	–	565	405	–	–	–	–	93	89	***	476	552	**	8.6	11.7	–	39.0	42.6	**
I140	16.2	16.9	–	22.2	23.0	–	267	373	–	14.9	11.2	***	75	73	–	622	645	–	7.4	10.1	–	34.5	36.4	*
Q103	15.7	16.3	–	21.4	21.9	–	339	444	–	16.1	14.3	***	89	86	*	555	578	–	6.6	9.1	–	35.0	37.1	*
Q163	16.0	16.7	–	22.0	22.9	–	356	481	–	–	–	–	92	89	–	636	668	–	6.6	8.5	–	35.0	36.3	–
Q251	12.2	12.6	–	17.3	18.1	–	504	617	–	29.9	27.1	**	91	88	*	605	665	*	9.3	11.4	–	40.1	43.3	*
Q361	16.7	17.3	–	21.8	22.8	–	309	319	–	9.7	6.5	***	84	80	**	724	729	–	9.3	10.9	–	36.4	37.9	–
Q401	14.8	15.1	–	21.0	21.2	–	526	495	–	30.7	28.5	***	88	86	–	594	614	–	9.1	8.6	–	38.3	37.9	–
Q521	13.8	15.0	**	17.9	19.6	***	435	325	–	21.6	13.7	***	87	79	***	614	642	–	7.0	10.9	–	36.6	41.0	***
All	14.8	15.4	***	20.2	21.0	***	3 301	3 460	–	20.4	16.7	***	87	84	***	604	637	***	8.0	10.1	**	36.9	39.1	***

*, **, ***Statistically significant difference between years 2021 and 2022 in meteorological and environmental parameters $P < 0.05$, $P < 0.01$, and $P < 0.001$

https://doi.org/10.17221/57/2024-JFS

Table 3. Incorporating the effects of meteorological and environmental conditions on stomatal conductance: The effects of temperature (f_{temp}), vapour pressure deficit (f_{VPD}), soil water (f_{SW}), and irradiance (f_{light}); parameters f_{temp}, f_{VPD}, f_{SW}, and f_{light} expressed as relative proportion functions, taking values between 0 and 1 as a proportion of the maximal stomatal conductance of *Fagus sylvatica* during the 2021 and 2022 vegetation seasons

Plot	f_{temp}			f_{VPD}			f_{SW}			f_{light}		
	2021	2022	*P*	2021	2022	*P*	2021	2022	*P*	2021	2022	*P*
B151	0.80	0.81	–	1.00	1.00	–	–	–	–	0.79	0.82	*
I140	0.90	0.88	–	1.00	0.99	–	0.82	0.54	***	0.88	0.87	–
Q103	0.90	0.89	–	1.00	1.00	–	0.99	0.82	***	0.86	0.85	–
Q163	0.90	0.88	–	1.00	1.00	–	–	–	–	0.88	0.87	–
Q251	0.77	0.79	–	1.00	1.00	–	1.00	0.89	***	0.86	0.86	–
Q361	0.90	0.88	–	1.00	0.99	–	0.57	0.79	***	0.91	0.90	–
Q401	0.86	0.87	–	1.00	1.00	–	0.98	1.00	**	0.85	0.84	–
Q521	0.88	0.85	–	1.00	0.98	–	1.00	0.67	***	0.87	0.87	–
All	0.86	0.87	–	1.00	1.00	–	0.98	1.00	**	0.86	0.86	–

*, **, ***Statistically significant difference in meteorological and environmental parameters $P < 0.05$, $P < 0.01$, and $P < 0.001$

recorded for the 2022 vegetation season, on average, across all stations and for two individual stations.

Significant differences were also found in *RAH* between the two vegetation seasons. Statistically significantly higher *RAH* values were generally observed during the 2021 vegetation season, which was also the case for eight individual plots. On average, across all plots, we also observed significantly higher soil moisture in 2021 and 2022 at a depth of 10 cm (as well as at 30 cm and 50 cm depths, data not shown) for all plots and, on average, across all plots. However, soil moisture data are available just for six out of eight plots. No significant differences were detected in total precipitation between 2021 and 2022, either in terms of average values across plots or at individual plots. To sum up the meteorological and environmental conditions, the 2021 vegetation season was characterised by lower temperatures and higher *RAH* and soil moisture in comparison to 2022.

We evaluated the meteorological and environmental conditions in terms of plant physiology of the most frequent symptomatic and O_3-sensitive *Fagus sylvatica* using the values of the parameters f_{temp}, f_{VPD}, f_{SW} and f_{light}. From these findings, we can conclude that the conditions for stomatal conductance, with the exception of soil moisture, were comparable in both the 2021 and 2022 vegetation seasons (Table 3). Soil moisture conditions were less favourable for stomatal conductance in 2022.

O_3 concentrations and AOT40F. The highest O_3 concentrations were observed at plots located at the highest altitude (940 m a.s.l.). A correlation between O_3 concentrations and altitude was found for both vegetation seasons (Figure 2). Significantly

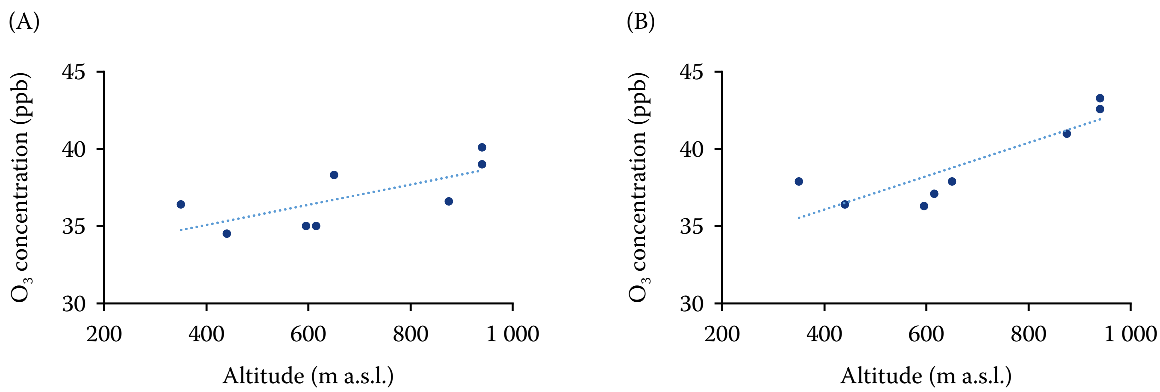

Figure 2. Relationships between O_3 concentration on altitude for the (A) 2021 and (B) 2022 vegetation seasons

rSp = 0.8, $P < 0.05$ for both evaluated years; *rSp* – Spearman's correlation coefficient

https://doi.org/10.17221/57/2024-JFS

higher O_3 concentrations were found during the 2022 vegetation season (Table 2).

The exposure index AOT40F was calculated for eight selected plots for the 2021 and 2022 vegetation seasons. In both vegetation seasons, the CL of AOT40F level (5 ppm·h^{-1}) was exceeded at all plots. The exceedance of the CL occurred in most cases before mid-July. In the 2021 season, AOT40F values ranged from approximately 6.6 ppm·h^{-1} to 9.3 ppm·h^{-1}. In the 2022 season, AOT40F values ranged from approximately 8.5 ppm·h^{-1} to 11.7 ppm·h^{-1} (Figure 3). The CL was exceeded at individual plots in the 2021 vegetation season by approximately 31% to 85% and in the 2022 season by 70% to 132%.

The AOT40F values were statistically significantly lower in the 2021 season (average: 8.0 ppm·h^{-1}) compared to the 2022 season (average: 10.1 ppm·h^{-1}; Table 2). No dependence of AOT40F values on altitude was found for either vegetation season.

Visible foliar O_3 injury. During the spring assessment in 2021, no symptoms of the negative effect of ground-level O_3 on the vegetation were detected on trees, shrubs or herbs, with the exception of the *Picea abies*, where symptoms were detected on 3-year-old and older needles. During the autumn evaluation in 2021, symptoms were detected on plot Q361 only on a few leaves of *Sambucus nigra* and *Fraxinus excelsior*. In the other plots, no symptoms of damage caused by increased concentrations of ground-level O_3 were detected.

In 2022, slightly more symptoms, identified as the O_3 effect, were observed than in 2021. Symptoms were detected on *Fagus sylvatica* in plots I140, Q163, Q251 and Q401. In the Q251 plot, the O_3 symptoms also manifested on *Rubus idaeus*. In the B151 plot, the effect of O_3 was observed on *Petasites albus*. Examples of visible foliar O_3 injury are shown in Figure 4.

During the 2022 vegetation season, the proportion of symptomatic species within individual plots ranged from 0% to 33%. The proportion of symptomatic squares within the LESS plots ranged from 0% to 12% (Table 4). No dependence was found between the percentage of symptomatic species and squares, respectively, on the O_3 concentration or AOT40 (Table 4).

The higher frequency of the occurrence of visible foliar O_3 injury during the 2022 vegetation season compared to 2021 may be caused by the colder start of season 2021 (Figure 5; CHMI 2022). Relatively low temperatures might have contributed to limited stomatal function and subsequently reduced O_3 accumulation. In terms of moisture conditions, a detailed analysis of monthly *RAH* and soil moisture indicates higher values in 2021. The analysis of f_{VPD} values indicated that *RAH* did not limit stomatal function during either the 2021 or 2022 vegetation seasons. Nevertheless, the analysis of f_{SW} values indicated and confirmed that soil moisture was lower and limited stomatal function mainly during vegetation season 2022 (Table 3). The more frequent occurrence of visible foliar O_3 injury in 2022 suggests that stomatal conductance limitation due to lower soil moisture was not crucial, and, in combination with higher O_3 concentrations in 2022, environ-

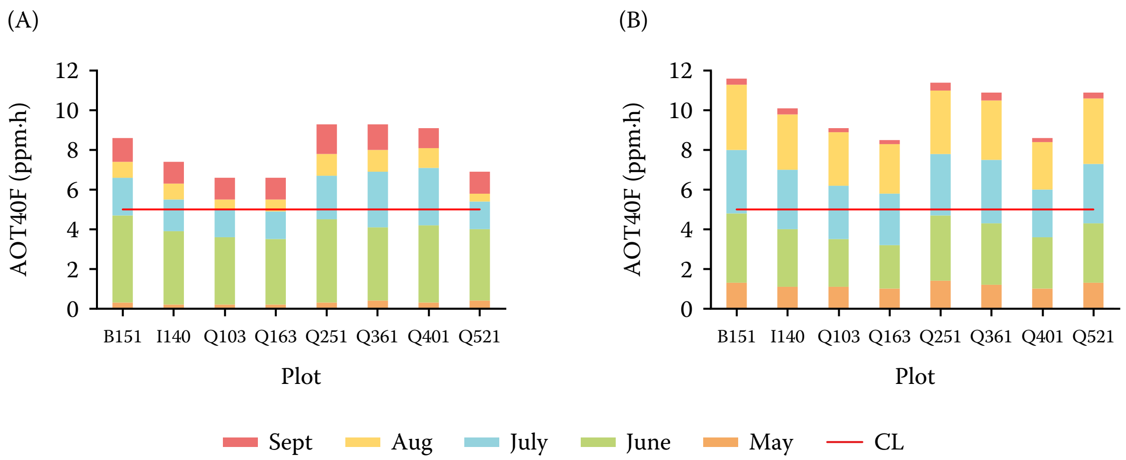

Figure 3. Contribution of monthly cumulated values of AOT40F to the total sum for the (A) 2021 and (B) 2022 vegetation seasons at monitoring plots

AOT40F – accumulated O_3 concentration over a threshold of 40 ppb for forest protection; CL – critical level

https://doi.org/10.17221/57/2024-JFS

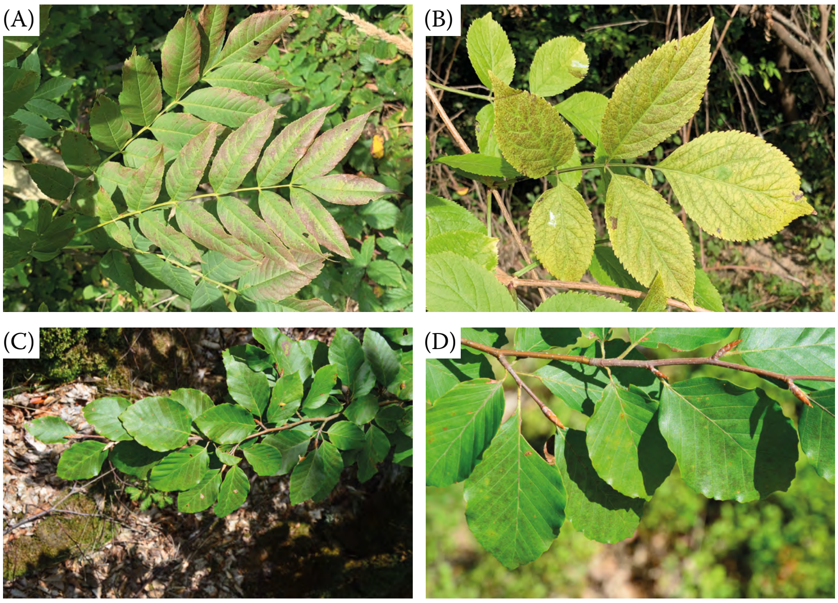

Figure 4. Examples of visible foliar O_3 injury on species within the LESS (light-exposed sampling site) plots in the 2021 and 2022 vegetation seasons: (A) *Fraxinus excelsior,* (B) *Sambucus nigra*, (C) and (D) *Fagus sylvatica*

Photos: Radek Novotný, Václav Buriánek

Table 4. A list of assessed and symptomatic species plus the percentage of symptomatic quadrates on the LESS (light-exposed sampling site) plots in 2021 and 2022

Plot code	Assessed woody species	Symptomatic species (%)				Symptomatic 2 × 1 m quadrates (%)	
		2021		2022		2021	2022
B151	*Acer pseudoplatanus, Fagus sylvatica, Fraxinus excelsior, Picea abies, Salix caprea, Sorbus aucuparia*	–	0	*Petasites albus*	14	0	6
I140	*Fagus sylvatica, Picea abies, Sorbus aucuparia*	–	0	*Fagus sylvatica*	33	0	12
Q103	*Alnus glutinosa, Betula pendula, Fagus sylvatica, Picea abies, Populus tremula, Quercus petraea, Salix caprea, Tilia cordata*	–	0	–	0	0	0
Q163	*Acer pseudoplatanus, Betula pendula, Fagus sylvatica, Frangula alnus, Picea abies, Pinus sylvestris, Populus tremula, Salix caprea*	–	0	*Fagus sylvatica*	13	0	9
Q251	*Acer pseudoplatanus, Alnus glutinosa, Betula pendula, Fagus sylvatica, Picea abies, Populus tremula, Salix aurita, Salix caprea, Salix cinerea, Sorbus aucuparia*	–	0	*Fagus sylvatica, Rubus idaeus*	20	0	9
Q361	*Acer campestre, Alnus glutinosa, Betula pendula, Cornus sanguinea, Corylus avellana, Fagus sylvatica, Fraxinus excelsior, Picea abies, Salix caprea, Sambucus nigra, Tilia cordata*	*Sambucus nigra, Fraxinus excelsior*	18	–	0	3	0
Q401	*Abies alba, Alnus glutinosa, Betula pendula, Fagus sylvatica, Picea abies, Populus tremula, Salix aurita, Salix caprea*	–	0	*Fagus sylvatica*	13	0	10
Q521	*Acer pseudoplatanus, Alnus glutinosa, Betula pendula, Fagus sylvatica, Fraxinus excelsior, Picea abies, Prunus* sp.*, Rosa canina, Salix aurita, Sambucus nigra, Sambucus racemosa, Sorbus aucuparia, Syringa* sp.	–	0	–	0	0	0

https://doi.org/10.17221/57/2024-JFS

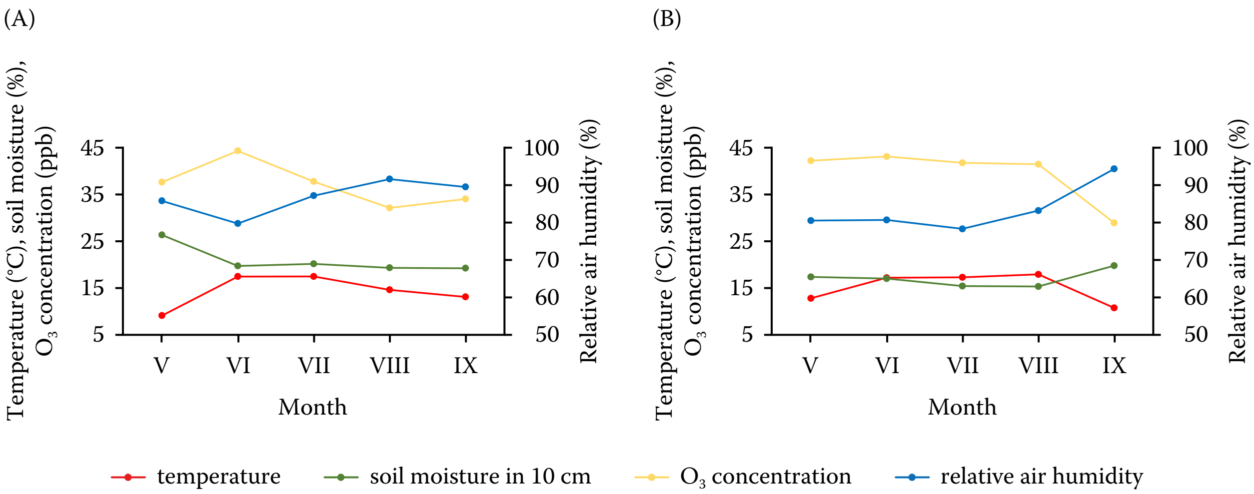

Figure 5. Temperature, relative air humidity, soil moisture, and O_3 concentration (monthly averages for all sites) during (A) the 2021 vegetation season and (B) the 2022 vegetation season

mental conditions were sufficient to cause visible O_3 leaf damage. Much higher O_3 concentrations occurred, particularly in July and August 2022.

MDA content. In our study, the content of MDA varied in leaves and needles from 3.99 $\mu mol \cdot g^{-1}$ to 9.20 $\mu mol \cdot g^{-1}$ (Figure 6). We found significant differences in the MDA content between *Fagus sylvatica* and *Picea abies* in 2021. For the year 2022, the test was non-significant. No significant difference was found in testing MDA content in 2021 and 2022. The analysis of *Fagus sylvatica* leaves separately, according to visible foliar O_3 injury evidence, showed that the MDA content was higher in damaged leaves in comparison to healthy leaves without any visible symptoms caused by visible foliar O_3 injury (Figure 7).

Multivariate analysis. The above analyses and assessments were complemented by a multiple-factor analysis for the vegetation season 2022, during which the presence of visible foliar O_3 injury was more frequent (Figure 8). The analysis indicates a correlation between rainfall and soil moisture, with positive correlations also observed among temperature parameters. From the multiple-factor analysis plot, it can be estimated that humidity (both air and soil) and temperature parameters together account for approximately 50% of the variance in O_3 foliar injury, expressed as the

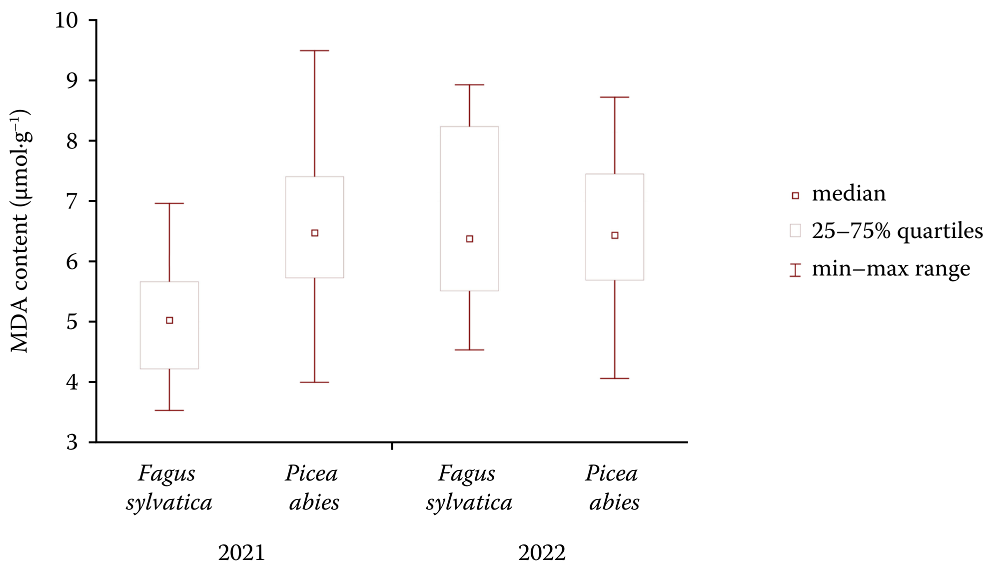

Figure 6. Malondialdehyde (MDA) content in *Fagus sylvatica* leaves and *Picea abies* needles in 2021 and 2022

https://doi.org/10.17221/57/2024-JFS

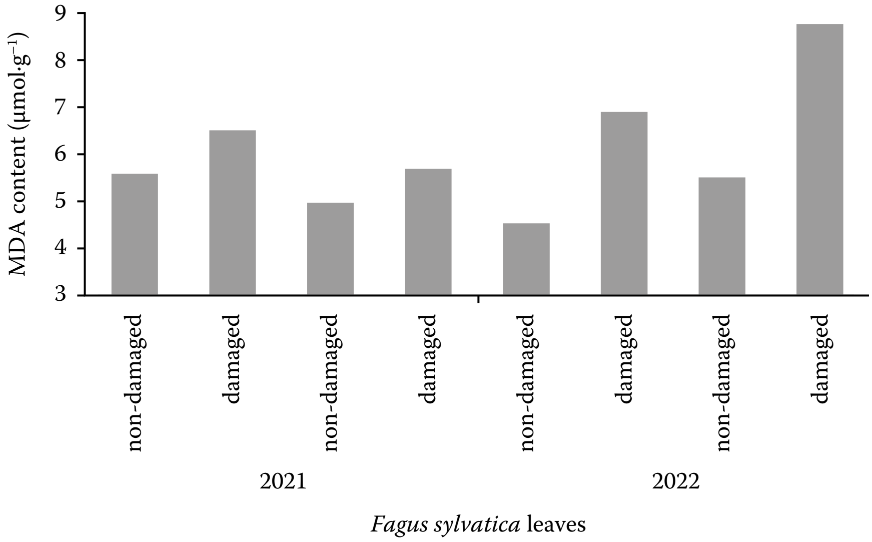

Figure 7. Comparison of the malondialdehyde (MDA) content in damaged and non-damaged *Fagus sylvatica* leaves

Pairs of damaged and non-damaged leaves were sampled within the same plot; in 2021, the first was from plot Q163 and the second pair was from plot I140, while in 2022, the first pair was from plot Q163 and the second pair was from plot Q401

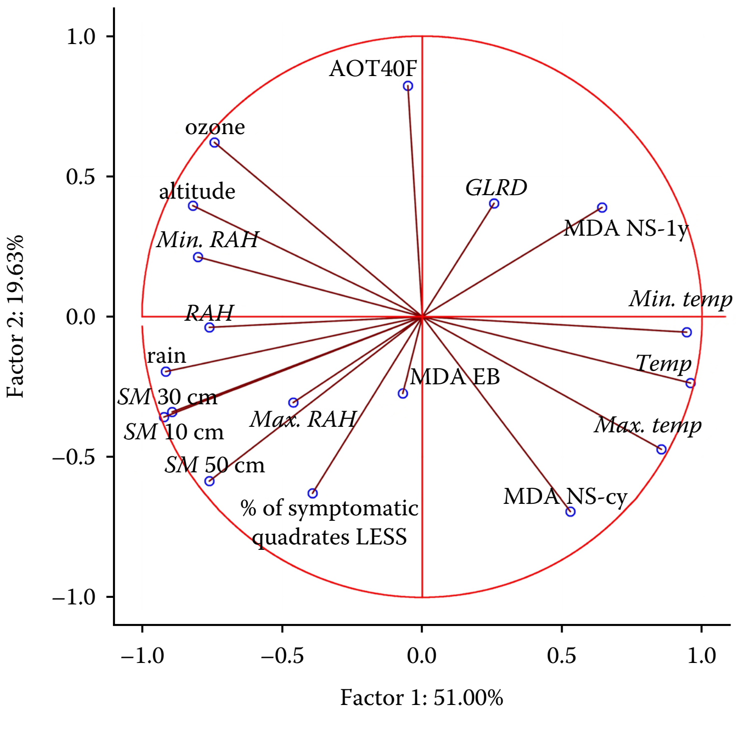

Figure 8. Multiple-factor analysis of meteorological and environmental variables within the percentage of symptomatic LESS (light-exposed sampling site) plots in the 2022 vegetation season

GLRD – global radiation; MDA NS-1y – malondialdehyde (MDA) content in one-year-old Norway spruce needles; *Min. temp* – minimal air temperature; *Temp* – average air temperature; *Max. temp* – maximal air temperature; MDA NS-cy – MDA content in current-year Norway spruce needles; MDA EB – MDA content in leaves of Europaean beach; LESS – light-exposed sampling site; *SM* – soil moisture; *Min. RAH* – minimal relative air humidity; *RAH* – average relative air humidity; *Max. RAH* – maximal relative air humidity; AOT40F – accumulated O_3 concentration over a threshold of 40 ppb for forest protection

https://doi.org/10.17221/57/2024-JFS

percentage of symptomatic LESS plots. In contrast, O_3 concentration and AOT40F contribute less to the variability of the percentage of symptomatic LESS plots. This confirms our assumption that O_3 foliar injury on vegetation is primarily observed in years or plots where gas exchange by stomatal closure is not crucially limited, while atmospheric O_3 concentrations are sufficient for plants to receive a phytotoxic dose. Additionally, the results do not confirm a correlation between O_3 concentration or AOT40 and the visible foliar O_3 injury on leaves and needles of trees.

DISCUSSION

Ground-level O_3 is still considered the most harmful air pollutant for vegetation (Feng et al. 2019; Anav et al. 2022). Furthermore, ground-level O_3 will continue to be problematic for ecosystems in the future because climate change will result in higher temperatures and higher emissions of methane, which is an O_3 precursor and will increase the global O_3 concentration (Meleux et al. 2007; The Royal Society 2008; Sicard et al. 2017). For this reason, surveys from real forest conditions are still necessary (Paoletti et al. 2022). Visible foliar injury is the first unequivocal symptom indicating phytotoxicity dose of O_3 (Bergmann et al. 1999) and can, therefore, be used to set critical levels for real-world forest protection (Paoletti et al. 2019). The monitoring of visible foliar injury (together with the estimation of exceedances of critical levels for POD for terrestrial ecosystems) to assess O_3 damage to vegetation growth and biodiversity is recommended by Annex V of Directive (EU) 2016/2284 on the reduction of national emissions of certain atmospheric pollutants (EP 2016) and by the Commission Notice on ecosystem monitoring under Article 9 and Annex V of Directive (EU) 2016/2284 (EC 2019; De Marco et al. 2019). Moreover, based on the proposal for a directive of the European Parliament and of the Council on ambient air quality and cleaner air for Europe (Article 8.8), it is very probable that 'the use of bioindicators shall be considered where regional patterns of the impact on ecosystems are to be assessed, including in accordance with the monitoring undertaken under Directive (EU) 2016/2284' (EU 2024).

When evaluating visible foliar O_3 injury, it is important to consider not only O_3 concentrations but also the meteorological and environmental parameters of the given vegetation season that are crucial for the stomatal conductance and O_3 dose absorbed by plants (Emberson et al. 2000; Matyssek et al. 2007; Anav et al. 2016; Bičárová et al. 2019). Based on the results of monitoring these parameters, we can conclude that the 2021 vegetation season was characterised by lower temperatures and higher *RAH* and soil moisture in comparison to 2022.

Regarding temperature, the 2021 vegetation season (May–September) was normal, with an average temperature of 15.7 °C, which was 0.1 °C below the normal of 1991–2020. The 2022 vegetation season was above normal, with an average annual temperature of 16.5 °C. In terms of precipitation, the 2021 vegetation season was above normal, with a total precipitation of 423 mm, corresponding to 112% of the normal of 1991–2020. In the 2022 vegetation season, precipitation levels remained within normal ranges, with a total precipitation of 387 mm, representing 102% of the 1991–2020 normal. In 2022, the months with below-normal precipitation were May (71% of normal) and July (70%), while in 2021, precipitation was only below normal in September (38% of normal) (CHMI 2022, 2023a). Therefore, it is possible to say that our meteorological observations are in agreement with the nationwide statistics of the Czech Hydrometeorological Institute, and our selected plots are representative of the Czech Republic.

The seasonal O_3 concentration average across the sites was 36.9 ppb and 39.1 ppb during the 2021 and 2022 vegetation seasons, respectively. This is within the scope of values reported by Hůnová et al. (2011) and Vlasáková-Matoušková and Hůnová (2015) for the 2006–2008 vegetation seasons, which ranged from 36.0 ppb to 41.1 ppb. The average AOT40F value across the plots was 8.0 $ppm{\cdot}h^{-1}$ and 10.1 $ppm{\cdot}h^{-1}$ during the 2021 and 2022 vegetation seasons, respectively. The effect of altitude on the increase of O_3 concentration values, which is generally accepted by many authors (Brodin et al. 2010; Bičárová et al. 2016; Dalstein, Ciriani 2019), was also demonstrated in the present study. On the other hand, the dependence of AOT40F values on altitude was not significant; the reason for this could be the relatively low O_3 concentration (a seasonal average of between 34.5 ppb and 43.3 ppb at individual plots), indicating that hourly O_3 concentration fluctuates around a threshold of 40 ppb and not all of the O_3 concentrations are

https://doi.org/10.17221/57/2024-JFS

accumulated for AOT40F. This is further evidence that the use of AOT40 is not suitable for evaluation since even O_3 concentrations below 40 ppb are harmful to vegetation (Sicard et al. 2016). Moreover, the vegetation at higher altitudes is more vulnerable not only due to higher O_3 concentration but also because of more favourable conditions for stomatal conductance (Wieser et al. 2000; Díaz-de-Quijano et al. 2009).

Compared to the values of AOT40F over the Czech forested area between 2000 and 2015 (Hůnová et al. 2019b), the AOT40F values calculated for our plots were relatively low. However, these values are not fully comparable because Hůnová et al. (2019b) calculated AOT40F for the period of April–September, but we assumed the beginning of the vegetation season to be mid-May. Moreover, as Vlasáková-Matoušková and Hůnová (2015) showed, the contribution of the April values to the total AOT40F value could be considerable (i.e. more than 15%).

Visible foliar O_3 injury occurred on our plots even at these lower AOT40F values. This was similar to findings by Vlasáková-Matoušková and Hůnová (2015), who observed visible foliar O_3 injury on *Fagus sylvatica* in the field at AOT40F values between 6.2 ppm·h^{-1} and 17 ppm·h^{-1}. Araminienė et al. (2019) also reported visible foliar O_3 injury on native forest vegetation in Lithuania at AOT40F values ranging from 5.3 ppm·h^{-1} to 13.6 ppm·h^{-1}.

Other than *Fagus sylvatica* and *Fraxinus excelsior*, which are considered to be O_3-sensitive species (Baumgarten et al. 2000; Sicard et al. 2016), we found visible foliar O_3 injury on *Sambucus nigra*, *Rubus idaeus*, and *Petasites albus*. The influence of O_3 on the most frequent sensitive species, *Fagus sylvatica*, was also evidenced by the higher MDA content in injured leaves in comparison to leaves without any visible symptoms caused by O_3. Unfortunately, MDA cannot be considered a unique biochemical marker indicating only the influence of O_3 because the MDA content reflects the entire spectrum of oxidative stressors, including drought periods (Šrámek et al. 2012).

The percentage of symptomatic species we found within the LESS plots (0–33%) can be compared with the study of Sicard et al. (2021), who found 0–28% of symptomatic species over the period from 2017 to 2019 in Italy, including four out of nine sites that contained more than 20% symptomatic species. Paoletti et al. (2019), who framed the MOTTLES forest site network across three countries (France, Italy, Romania) and four biogeographical regions (Atlantic, Continental, Mediterranean, Alpine), identified 0–50% of symptomatic species on individual LESS plots in 2017. The percentage of symptomatic quadrats is lower (0–12%) compared to an earlier study from the Jizera Mountains (Vlasáková-Matoušková, Hůnová 2015), where the findings showed up to 55% of symptomatic quadrats targeting *Fagus sylvatica*. Manzini et al. (2023) evaluated even up to 100% of symptomatic quadrats focused on *Fagus sylvatica*. However, these were sites in the Alpine biome above 1 000 m, where both high O_3 concentrations and conditions suitable for O_3 uptake can be expected.

We did not find the dependence of visible foliar O_3 injury (expressed as a percentage of symptomatic quadrats in LESS plots or a percentage of symptomatic species) on AOT40F. This is consistent with many previous studies that did not find a correlation between O_3 injury and exposure indices or that indicated that O_3 exposure was not an accurate predictor of visible foliar O_3 injury (Matyssek et al. 2007; Hoshika et al. 2011; Anav et al. 2019; Araminienė et al. 2019; Paoletti et al. 2019). The reasons for the occurrence and extent of visible O_3 foliar injury must, therefore, be sought not only in O_3 concentration levels but also in meteorological and environmental conditions on plots (especially soil moisture) that affect stomatal opening and O_3 uptake by vegetation (Araminienė et al. 2019; Bičárová et al. 2019; Sicard et al. 2021; Moura et al. 2022).

Sicard et al. (2016) highlighted that the most important environmental variable affecting visible O_3 injury in all tree species was soil water content, while the annual O_3 concentrations had the lowest relative importance. Similar findings were confirmed by multiple factorial analyses for 2022 for our plots when there was a development of visible foliar O_3 injury. Our results show that soil parameters, as determined by both soil moisture and f_{SW} parameters, were less favourable for stomatal conductance in 2022. However, the more frequent occurrence of visible foliar O_3 injury in 2022 confirmed that in combination with higher O_3 concentrations, it was sufficient for its occurrence. Without more detailed stomatal flux analysis and POD calculation, we can only assume that there was not enough O_3 accumulation in 2021, a year with more favourable soil conditions, to cause O_3 symptoms. This is also suggested by the CHMI (2023b) analysis,

https://doi.org/10.17221/57/2024-JFS

which indicates that 2021 had the lowest O_3 concentrations of the 2012–2022 assessment period.

Other reasons for the relative rareness of visible O_3 foliar injury in our plots could be the plant detoxification system or the natural genetic variability within the same species (Matyssek, Sandermann 2003; Vollenweider et al. 2003). However, our considerations are not fully supported by the observations on plot I140 in 2022, which had the least favourable soil moisture conditions (average f_{sw} = 0.54, average soil moisture content = 11.2%) but also the greatest vegetation damage. An explanation can be found in the study by Moura et al. (2022). They highlight a phenomenon where drought aggravated the effect of O_3 concentrations on visible leaf injury on *Quercus pubescens* leaves, which were not protected from severe oxidative stress, as the combination of O_3 and drought altered the activity of the antioxidant system.

In summary, this study suggests that the impact of ground-level O_3 on vegetation was relatively less pronounced as assessed by the visible foliar O_3 symptoms. However, the monitoring of O_3-induced visible injury represents the initial step in identifying potential health issues within forest ecosystems that may require further investigation (Coulston et al. 2003). Visible foliar O_3 injury can lead to reduced growth, increased defoliation, decreased productivity, and significant consequences at the ecosystem level (Paoletti et al. 2019; Manzini et al. 2023).

CONCLUSION

The study presents the results of the mapping of O_3 impact on vegetation for two vegetation seasons: 2021 and 2022. In contrast to the relatively high phytotoxic potential expressed by the AOT40F index, visible foliar O_3 injury was relatively rare. Our results confirm the widely accepted fact that the AOT40 exposure index is not an adequate tool for assessing the phytotoxic effects of O_3 on vegetation. Addressing this issue requires a more comprehensive approach that integrates the analysis of biologically meaningful visible symptoms and environmental conditions.

Results from eight monitored plots show a relevant influence of soil and meteorological conditions on the development and presence of visible foliar symptoms on leaves of woody species. The two vegetation seasons evaluated differed significantly in soil moisture and O_3 levels, leading to different results in visible foliar symptoms. In agreement with many studies, altitude effect on O_3 concentration was found, which is often associated with greater vegetation damage at higher altitudes where conditions are favourable for stomatal flux.

Visible foliar O_3 injury was more common in 2022, suggesting that environmental conditions, including less favourable soil moisture, together with higher O_3 concentrations compared to 2021, were sufficient to cause injury. The results highlight the importance of monitoring and managing O_3 pollution and its effects on vegetation, especially under changing climatic conditions, and confirm the need to work on POD-based critical levels for O_3 in the future. In conclusion, we advocate that our work from real field conditions contributes to forest protection regulations, which should be based on visible O_3 foliar injury and stomatal flux rather than O_3 exposure alone.

REFERENCES

Agathokleous E., Feng Z., Oksanen E., Sicard P., Wang Q., Saitanis C.J., Araminiene V., Blande J.D., Hayes F., Calatayud V., Domingos M., Veresoglou S.D., Peñuelas J., Wardle D.A., De Marco A., Li Z., Harmens H., Yuan X., Vitale M., Paoletti E. (2020): Ozone affects plant, insect, and soil microbial communities: A threat to terrestrial ecosystems and biodiversity. Science Advances, 6: 1–17.

Ainsworth E.A. (2016): Understanding and improving global crop response to ozone pollution. The Plant Journal, 90: 886–897.

Anav A., De Marco A., Proietti C., Alessandri A., Dell'Aquila A., Cionni I., Friedlingstein P., Khvorostyanov D., Menut L., Paoletti E., Sicard P., Sitch S., Vitale M. (2016): Comparing concentration-based (AOT40) and stomatal uptake (PODY) metrics for ozone risk assessment to European forests. Global Change Biology, 22: 1608–1627.

Anav A., De Marco A., Friedlingstein P., Savi F., Sicard P., Sitch S., Vitale M., Paoletti E. (2019): Growing season extension affects ozone uptake by European forests. Science of the Total Environment, 669: 1043–1052.

Anav A., De Marco A., Collalti A., Emberson L., Feng Z., Lombardozzi D., Sicard P., Verbeke T., Viovy N., Vitale M., Paoletti E. (2022): Legislative and functional aspects of different metrics used for ozone risk assessment to forests. Environmental Pollution, 295: 118690.

Araminienė V., Sicard P., Anav A., Agathokleous E., Stakėnas V., De Marco A., Varnagirytė-Kabašinskienė I., Paoletti E., Girgždienė R. (2019): Trends and inter-relationships

https://doi.org/10.17221/57/2024-JFS

of ground-level ozone metrics and forest health in Lithuania. Science of the Total Environment, 666: 1265–1277.

Ashmore M.R. (2003): Surface ozone effects on vegetation. In: Holton J.R., Curry J.A., Pyle J.A. (eds): Encyclopedia of Atmospheric Sciences. London, Elsevier Science: 1663–1671.

Ashmore M.R. (2005): Assessing the future global impacts of ozone on vegetation. Plant, Cell and Environment, 28: 949–964.

Baumgarten M., Werner H., Häberle K.H., Emberson L.D., Fabian P., Matyssek R. (2000): Seasonal ozone response of mature beech trees (*Fagus sylvatica*) at high altitude in the Bavarian forest (Germany) in comparison with young beech grown in the field and in phytotrons. Environmental Pollution, 108: 431–442.

Bergmann E., Bender J., Weigel H.J. (1999): Ozone threshold doses and exposure-response relationships for the development of ozone injury symptoms in wild plant species. New Phytologist, 144: 423–435.

Bičárová S., Sitková Z., Pavlendová H. (2016): Ozone phytotoxicity in the Western Carpathian Mountains in Slovakia. Forestry Journal, 62: 77–88. Available at: https://intapi.sciendo.com/pdf/10.1515/forj-2016-0008

Bičárová S., Sitková Z., Pavlendová H., Fleischer P.Jr., Fleischer P.Sr., Bytnerowicz A. (2019): The role of environmental factors in ozone uptake of *Pinus mugo* Turra. Atmospheric Pollution Research, 10: 283–293.

Boháčová L., Lomský B., Šrámek V. (2011): Development of the Monitoring of Forest Health State Under Life+ 'FutMon' project in the Czech Republic. Strnady, Forestry and Game Management Research Institute: 58. Available at: https://invenio.nusl.cz/record/432014/files/nusl-432014_1.pdf

Brodin M., Helmig D., Oltmans S.J. (2010): Seasonal ozone behavior along an elevation gradient in the Colorado Front Range Mountains. Atmospheric Environment, 44: 5305–5315.

Carrari E., Dalstein L., Hoshika Y., Paoletti E. (2020): MOTTLES Atlas of Visible Foliar Ozone Injury. Available at: https://mottles-project.wixsite.com/life/atlas-ozone-injury

CHMI (2022): Klimatologická ročenka České republiky 2021. Prague, Czech Hydrometeorological Institute: 84. Available at: https://info.chmi.cz/rocenka/meteo2021/meteo2021_SQ.pdf (in Czech).

CHMI (2023a): Klimatologická ročenka České republiky republiky 2022. Prague, Czech Hydrometeorological Institute: 84. Available at: https://info.chmi.cz/rocenka/meteo2022/meteo2022_SQ.pdf (in Czech).

CHMI (2023b): Znečištění ovzduší na území České republiky v roce 2022. Prague, Czech Hydrometeorological Institute: 182. Available at: https://www.chmi.cz/files/portal/docs/uoco/isko/grafroc/22groc/gr22cz/UKO_Rocenka_2022_v3.pdf (in Czech).

Cieslik S. (2009): Ozone fluxes over various plant ecosystems in Italy: A review. Environmental Pollution, 157: 1487–1496.

CLRTAP (2017): Chapter III: Mapping critical levels for vegetation. In: Manual for Modelling and Mapping Critical Loads and Levels. UNECE Convention on Long Range Transboundary Air Pollution: 66. Available at: https://icpvegetation.ceh.ac.uk/sites/default/files/FinalnewChapter3v4Oct2017_000.pdf

Coates J., Mar K.A., Ojha N., Butler T.M. (2016): The influence of temperature on ozone production under varying NO_X conditions – A modelling study. Atmospheric Chemistry and Physics, 16: 11601–11615.

Coulston J.W., Smith G.C., Smith W.D. (2003): Regional assessment of ozone sensitive tree species using bioindicator plants. Environmental Monitoring and Assessment, 83: 113–127. Available at: https://link.springer.com/article/10.1023/A:1022578506736

Cox W.M., Chu S. (1993): Meteorologically adjusted ozone trends in urban areas: A probabilistic approach. Atmospheric Environment. Part B. Urban Atmosphere, 27: 425–434.

Dalstein L., Ciriani M.L. (2019): Ozone foliar damage and defoliation monitoring of *P. cembra* between 2000 and 2016 in the southeast of France. Environmental Pollution, 244: 451–461.

Davey M.W., Stals E., Panis B., Keulemans J., Swennen R.L. (2005): High-throughput determination of malondialdehyde in plant tissues. Analytical Biochemistry, 347: 201–207.

De Marco A., Vitale M., Popa I., Anav A., Badea O., Silaghi D., Leca S., Screpanti A., Paoletti E. (2017): Ozone exposure affects tree defoliation in a continental climate. Science of the Total Environment: 369–404.

De Marco A., Proietti C., Anav A., Ciancarella L., D'Elia I., Fares S., Fornasier M.F., Fusaro L., Gualtieri M., Manes F., Marchetto A., Mircea M., Paoletti E., Piersanti A., Rogora M., Salvati L., Salvatori E., Screpanti A., Vialetto G., Vitale M., Leonardi C. (2019): Impacts of air pollution on human and ecosystem health, and implications for the National Emission Ceilings Directive: Insights from Italy. Environment International, 125: 320–333.

Díaz-de-Quijano M., Peñuelas J., Ribas À. (2009): Increasing interannual and altitudinal ozone mixing ratios in the Catalan Pyrenees. Atmospheric Environment, 43: 6049–6057.

EC (2019): Communication from the Commission – Commission Notice on ecosystem monitoring under Article 9 and Annex V of Directive (EU) 2016/2284 of the European Parliament and of the Council on the reduction of national emissions of certain atmospheric pollutants (NEC-Directive). European Commission. Available at: https://eur-lex.europa.eu/legal-content/EN/ALL/?uri=oj:JOC_2019_092_R_0001

https://doi.org/10.17221/57/2024-JFS

EEA (2020): Air Quality in Europe — 2020 Report. EEA Report No. 9/2020. Luxembourg, European Environment Agency: 160. Available at: https://www.eea.europa.eu/publications/air-quality-in-europe-2020-report

Emberson L.D., Ashmore M.R., Cambridge H.M., Simpson D., Tuovinen J.P. (2000): Modelling stomatal ozone flux across Europe. Environmental Pollution, 109: 403–413.

Emberson L.D., Pleijel H., Ainsworth E.A., van den Berg M., Ren W., Osborne S., Mills G., Pandey D., Dentener F., Büker P., Ewert F., Koeble R., Van Dingenen R. (2018): Ozone effects on crops and consideration in crop models. European Journal of Agronomy, 100: 19–34.

EP (2008): Directive 2008/50/EC of the European Parliament and of the Council of 21 May 2008 on ambient air quality and cleaner air for Europe. European Parliament, Council of the European Union. Available at: https://eur-lex.europa.eu/legal-content/EN/TXT/?uri=CELEX%3A32008L0050

EP (2016): Directive (EU) 2016/2284 of the European Parliament and of the Council of 14 December 2016 on the reduction of national emissions of certain atmospheric pollutants, amending Directive 2003/35/EC and repealing Directive 2001/81/EC. European Parliament, Council of the European Union. Available at: http://data.europa.eu/eli/dir/2016/2284/oj

EU (2024): Directive (EU) 2024/2881 of the European Parliament and of the Council of 23 October 2024 on ambient air quality and cleaner air for Europe (recast). European Parliament, Council of the European Union. Available at: https://eur-lex.europa.eu/legal-content/EN/TXT/?uri=CELEX%3A32024L2881

Fares S., Matteucci G., Scarascia Mugnozza G., Morani A., Calfapietra C., Salvatori E., Fusaro L., Manes F., Loreto F. (2013): Testing of models of stomatal ozone fluxes with field measurements in a mixed Mediterranean forest. Atmospheric Environment, 67: 242–251.

Fares S., Conte A., Chabbi A. (2017): Ozone flux in plant ecosystems: New opportunities for long-term monitoring networks to deliver ozone-risk assessments. Environmental Science and Pollution Research, 25: 8240–8248.

Feng Z., De Marco A., Anav A., Gualtieri M., Sicard P., Tian H., Fornasier F., Tao F., Guo A., Paoletti E. (2019): Economic losses due to ozone impacts on human health, forest productivity and crop yield across China. Environment International, 131: 104966.

Fuhrer J. (2002): Ozone impacts on vegetation. Ozone: Science & Engineering, 24: 69–74.

Heath R.L. (2008): Modification of the biochemical pathways of plants induced by ozone: What are the varied routes to change? Environmental Pollution, 155: 453–463.

Heath R.L, Packer L. (1968): Photoperoxidation in isolated chloroplasts. Archives of Biochemistry and Biophysics, 125: 189–198.

Horálek J., Vlasáková L., Schreiberová M., Benešová N., Schneider P., Kurfürst P., Tognet F., Schovánková J., Vlček O., Vivanco M.G., Theobald M., Gil V. (2023). Air quality maps of EEA member and cooperating countries for 2021. PM_{10}, $PM_{2.5}$, O_3, NO_2, NO_x and BaP spatial estimates and their uncertainties (Eionet Report – ETC HE 2023/3). European Topic Centre on Human Health and the Environment: 129. Available at: https://zenodo.org/records/10589987

Hoshika Y., Shimizu Y., Omasa K. (2011): A comparison between stomatal ozone uptake and AOT40 of deciduous trees in Japan. iForest – Biogeosciences and Forestry, 4: 128–135.

Hoshika Y., Watanabe M., Inada N., Mao Q., Koike T. (2013): Photosynthetic response of early and late leaves of white birch (*Betula platyphylla* var. *japonica*) grown under free-air ozone exposure. Environmental Pollution, 182: 242–247.

Hůnová I., Schreiberová M. (2012): Ambient ozone phytotoxic potential over the Czech forests as assessed by AOT40. iForest – Biogeosciences and Forestry, 5: 153–162.

Hůnová I., Bäumelt V. (2018): Observation-based trends in ambient ozone in the Czech Republic over the past two decades. Atmospheric Environment, 172: 157–167.

Hůnová I., Novotný R., Uhlířová H., Vráblík T., Horálek J., Lomský B., Šrámek V. (2010): The impact of ambient ozone on mountain spruce forests in the Czech Republic as indicated by malondialdehyde. Environmental Pollution, 158: 2393–2401.

Hůnová I., Matoušková L., Srněnský R., Koželková K. (2011): Ozone influence on native vegetation in the Jizerske hory Mts. of the Czech Republic: Results based on ozone exposure and ozone-induced visible symptoms. Environmental Monitoring and Assessment, 183: 501–515.

Hůnová I., Brabec M., Malý M. (2019a): What are the principal factors affecting ambient ozone concentrations in Czech mountain forests? Frontiers in Forests and Global Change, 2: 1–13.

Hůnová I., Kurfürst P., Baláková L. (2019b): Areas under high ozone and nitrogen loads are spatially disjunct in Czech forests. Science of the Total Environment, 656: 567–575.

Innes J.L., Skelly J.M., Schaub M. (2001): Ozone and Broadleaved Species: A Guide to the Identification of Ozone-induced Foliar Injury. Bern, Haupt: 136.

Jacob D.J., Winner D.A. (2009): Effect of climate change on air quality. Atmospheric Environment, 43: 51–63.

Jacob D.J., Logan J.A., Gardner G.M., Yevich R.M., Spivakovsky C.M., Wofsy S.C., Sillman S., Prather M.J. (1993): Factors regulating ozone over the United States and its export to the global atmosphere. Journal of Geophysical Research, 98: 14 817–14826.

https://doi.org/10.17221/57/2024-JFS

Manzini J., Hoshika Y., Baesso Moura B., Paoletti E. (2023): Exploring a new O_3 index as a proxy for the avoidance/tolerance capacity of forest species to tolerate O_3 injury. Forests, 14: 901–918.

Matyssek R., Sandermann H.Jr. (2003): Impact of ozone on trees: An ecophysiological perspective. Progress in Botany, 64: 349–404.

Matyssek R., Bytnerowicz A., Karlsson P.E., Paoletti E., Sanz M., Schaub M., Wieser G. (2007): Promoting the O_3 flux concept for European forest trees. Environmental Pollution, 146: 587–607.

Meleux F., Solmon F., Giorgi F. (2007): Increase in summer European ozone amounts due to climate change. Atmospheric Environment, 41: 7577–7587.

Mills G., Pleijel H., Malley C.S., Sinha B., Cooper O.R., Schultz M.G., Neufeld H.S., Simpson D., Sharps K., Feng Z., Gerosa G., Harmens H., Kobayashi K., Saxena P., Paoletti E., Sinha V., Xu X. (2018): Tropospheric ozone assessment report: Present-day tropospheric ozone distribution and trends relevant to vegetation. Elementa: Science of the Anthropocene, 6: 47.

Mittler R. (2002): Oxidative stress, antioxidants and stress tolerance. Trends in Plant Science, 7: 405–410.

Monks P.S. (2000): A review of the observations and origins of the spring ozone maximum. Atmospheric Environment, 34: 3545–3561.

Moura B.B., Paoletti E., Badea O., Ferrini F., Hoshika Y. (2022): Visible foliar injury and ecophysiological responses to ozone and drought in oak seedlings. Plants, 11: 1836.

Nolle M., Ellul R., Heinrich G., Güsten H. (2002): A long-term study of background ozone concentrations in the central Mediterranean – Diurnal and seasonal variations on the island of Gozo. Atmospheric Environment, 36: 1391–1402.

Novotný R., Buriánek V., Šrámek V. (2009): Metodika hodnocení viditelného poškození vegetace vyvolaného účinky přízemního ozonu. Lesnický průvodce 6. Strnady, Forestry and Game Management Research Institute: 48. Available at: https://www.vulhm.cz/files/uploads/2019/03/lp_2009_06.pdf (in Czech).

Novotný R., Šrámek V., Buriánek V. (2010): Evaluation of the ozone injury to ground vegetation within the plots of intensive monitoring in the Czech Republic. Lesnícky časopis – Forestry Journal, 56: 57–67. Available at: http://fj.nlcsk.org/images/pdf/Rocnik_56/Cislo_1_2010/Novotny_akol.pdf

Paoletti E., Alivernini A., Anav A., Badea O., Carrari E., Chivulescu S., Conte A., Ciriani M.L., Dalstein-Richier L., De Marco A., Fares S., Fasano G., Giovannelli A., Lazzara M., Leca S., Materassi A., Moretti V., Pitar D., Popa I., Sabatini F., Salvati L., Sicard P., Sorgi T., Hoshika Y. (2019): Toward stomatal–flux based forest protection against ozone: The MOTTLES approach. Science of the Total Environment, 691: 516–527.

Paoletti E., Sicard P., Hoshika Y., Fares S., Badea O., Pitar D., Popa I., Anav A., Baesso Moura B., De Marco A. (2022): Towards long-term sustainability of stomatal ozone flux monitoring at forest sites. Sustainable Horizons, 2: 100018.

Pell E.J., Schlagnhaufer C.D., Arteca R.N. (1997): Ozone-induced oxidative stress: Mechanisms of action and reaction. Physiologia Plantarum, 100: 264–273.

Raspe S., Fleck S., Beuker E., Preuhsler T., Bastrup-Birk A. (2020): Meteorological measurements. Version 2020-1. In: UNECE ICP Forests, Programme Co-ordinating Centre (ed.): Manual on Methods and Criteria for Harmonized Sampling, Assessment, Monitoring and Analysis of the Effects of Air Pollution on Forests. Eberswalde, Thünen Institute of Forest Ecosystems: 39. Available at: https://www.icp-forests.org/pdf/manual/2020/ICP_Manual_part09_2020_Meteorology_version_2020-1.pdf

R Core Team (2020): R: A Language and Environment for Statistical Computing. Vienna, R Foundation for Statistical Computing. Available at: https://www.R-project.org/

Reif J., Gamero A., Flosek J., Hůnová I. (2023): Ambient ozone – New threat to birds in mountain ecosystems? Science of the Total Environment, 876: 162711.

Schaub M., Calatayud V. (2013): Assessment of visible foliar injury induced by ozone. Developments in Environmental Science, 12: 205–221.

Schaub M., Skelly J.M., Zhang J.W., Ferdinand J.A., Savage J.E., Stevenson R.E., Davis D.D., Steiner K.C. (2005): Physiological and foliar symptom response in the crowns of *Prunus serotina*, *Fraxinus americana* and *Acer rubrum* canopy trees to ambient ozone under forest conditions. Environmental Pollution, 133: 553–567.

Schaub M., Calatayud V., Ferretti M., Brunialti G., Lövblad G., Krause G., Sanz M.J., Pitar D., Gottardini E. (2020): Part VIII: Assessment of ozone injury. Version 2020-1. In: UNECE ICP Forests Programme Co-ordinating Centre (ed.): Manual on Methods and Criteria for Harmonized Sampling, Assessment, Monitoring and Analysis of the Effects of Air Pollution on Forests. Eberswalde, Thünen Institute of Forest Ecosystems: 15 + Annex. Available at: https://www.icp-forests.org/pdf/manual/2020/ICP_Manual_part08_2020_Ozone_version_2020-1.pdf

Schraudner M., Langebartels C., Sandermann H. (1997): Changes in the biochemical status of plant cells induced by the environmental pollutant ozone. Physiologia Plantarum, 100: 274–280.

Sicard P., De Marco A., Dalstein-Richier L., Tagliaferro F., Renou C., Paoletti E. (2016): An epidemiological assessment of stomatal ozone flux-based critical levels for visible

https://doi.org/10.17221/57/2024-JFS

ozone injury in Southern European forests. Science of the Total Environment, 541: 729–741.

Sicard P., Anav A., De Marco A., Paoletti E. (2017): Projected global ground-level ozone impacts on vegetation under different emission and climate scenarios. Atmospheric Chemistry and Physics, 17: 12177–12196.

Sicard P., Hoshika Y., Carrari E., De Marco A., Paoletti E. (2021): Testing visible foliar injury within a light exposed sampling site as a proxy for ozone risk assessment for European forests. Journal of Forestry Research, 32: 1351–1359.

Šrámek V., Novotný R., Bednárová E., Uhlířová H. (2007): Monitoring of ozone risk for forests in the Czech Republic: Preliminary results. The Scientific World Journal, 7: 78–83.

Šrámek V., Novotný R., Vejpustková M., Hůnová I., Uhlířová H. (2012): Monitoring of ozone effects on the vitality and increment of Norway spruce and European beech in the Central European forests. Journal of Environmental Monitoring, 14: 1696–1702.

The Royal Society (2008): Ground-level Ozone in the 21st Century: Future Trends, Impacts and Policy Implications. RS Policy Document 15/08. London, The Royal Society: 131. Available at: https://royalsociety.org/-/media/policy/publications/2008/7925.pdf

Uhlířová H. (1991): Is it possible to use malondialdehyde content to damage assessment? In: IUFRO and ICP Forests Workshop on Monitoring Air Pollution Impact on Permanent Sample Plots, Data Processing and Results Interpretation, Prachatice, Sept 2–6, 1991: 233–235.

Uhlířová H., Pasuthová J. (1993): Diagnostics of latent air pollution damage to tree species. Lesnictví-Forestry, 39: 73–79.

Vingarzan R. (2004): A review of surface ozone background levels and trends. Atmospheric Environment, 38: 3431–3442.

Vlasáková-Matoušková L., Hůnová I. (2015): Stomatal ozone flux and visible leaf injury in native juvenile trees of *Fagus sylvatica* L.: A field study from the Jizerské hory Mts., the Czech Republic. Environmental Science and Pollution Research, 22: 10034–10046.

Vollenweider P., Ottiger M., Günthardt-Goerg M.S. (2003): Validation of leaf ozone symptoms in natural vegetation using microscopical methods. Environmental Pollution, 124: 101–118.

Wieser G., Häsler R., Götz B., Koch W., Havranek W.M. (2000): Role of climate, crown position, tree age, and altitude in calculated ozone flux into needles of *Picea abies* and *Pinus cembra*: A synthesis. Environmental Pollution, 109: 415–422.

Wittig V.E., Ainsworth E.A., Naidu S.L., Karnosky D.F., Long S.P. (2009): Quantifying the impact of current and future tropospheric ozone on tree biomass, growth, physiology and biochemistry: A quantitative meta-analysis. Global Change Biology, 15: 396–424.

Received: August 9, 2024
Accepted: November 21, 2024
Published online: January 24, 2025